



Article

Dual Crosslinked Gelatin Methacryloyl Hydrogels for Photolithography and 3D Printing

Gozde Basara, Xiaoshan Yue and Pinar Zorlutuna *

Aerospace and Mechanical Engineering Department, University of Notre Dame, Notre Dame, IN 46556, USA * Correspondence: Pinar.Zorlutuna.1@nd.edu; Tel.: +1-574-631-8543

Received: 29 April 2019; Accepted: 1 July 2019; Published: 3 July 2019



Abstract: Gelatin methacryloyl (GelMA) hydrogels have been used in tissue engineering and regenerative medicine because of their biocompatibility, photopatternability, printability, and tunable mechanical and rheological properties. However, low mechanical strength limits their applications in controlled drug release, non-viral gene therapy, and tissue and disease modeling. In this work, a dual crosslinking method for GelMA is introduced. First, photolithography was used to pattern the gels through the crosslinking of methacrylate incorporated amine groups of GelMA. Second, a microbial transglutaminase (mTGase) solution was introduced in order to enzymatically crosslink the photopatterned gels by initiating a chemical reaction between the glutamine and lysine groups of the GelMA hydrogel. The results showed that dual crosslinking improved the stiffness and rheological properties of the hydrogels without affecting cell viability, when compared to single crosslinking with either ultraviolet (UV) exposure or mTGase treatment. Our results also demonstrate that when treated with mTGase, hydrogels show decreased swelling properties and better preservation of photolithographically patterned shapes. Similar effects were observed when three dimensional (3D) printed and photocrosslinked substrates were treated with mTGase. Such dual crosslinking methods can be used to improve the mechanical properties and pattern fidelity of GelMA gels, as well as dynamic control of the stiffness of tissue engineered constructs.

Keywords: dual crosslinking; photocrosslinking; enzymatic crosslinking; microbial transglutaminase; photolithography; 3D printing

1. Introduction

The extracellular matrix (ECM) is the combination of molecules that provide structure and stability to biological tissues. In the realm of tissue engineering, biologically active scaffolds serve to mimic the native ECM [1–3]. ECM properties vary based on their biological functions, so it is crucial to develop scaffolds with adjustable chemical and mechanical properties in order to manipulate cell behavior [4]. Various types of natural and synthetic materials were used to create such scaffolds [5–8]. Gelatin methacryloyl (GelMA), a photocrosslinkable hydrogel obtained by modifying gelatin, is one of the most attractive materials due to its biocompatibility, tunable rheological and mechanical properties, low cost and printability [9,10]. Moreover, photopatterning can be used to fabricate micropatterned GelMA scaffolds [9,11,12]. However, its relatively poor mechanical properties, especially in the low concentrations frequently used for better cell viability [9,13–15] as well as improved cell spreading and migration [9], can be a limitation for tissue engineering applications where high ECM stiffness is required [16].

Existing strategies to improve the mechanical properties of GelMA gels usually involve the introduction of other materials. Biopolymers such as dextran [17], silk fibroin [18], hyaluronic acid, [19] and gellan gum [20] have been incorporated into GelMA gels to tune their mechanical properties. In addition, reinforcement with 3D printed carbon nano-tubes [21,22], microfibers [16],

polyacrylamide [23], graphene oxide [24], polyethylene glycol [25,26] and polylactide-co-ethylene oxide-co-fumarate (PLEOF) have been reported to alter the physical properties of GelMA gels. Introducing another material into GelMA hydrogels could require tedious processes, and more importantly cannot be done in a dynamic fashion. For example, to study the myocardial infarction in vitro, dynamic stiffening of the engineered hydrogels introduced by enzymatic crosslinking will be valuable, since it is shown that the tissue becomes stiffer after myocardial infarction [27]. This feature can also be used to study the effect of gradual stiffening of the substrate on breast cancer cells, as it is shown that the tissue ECM often stiffens when cancer occurs [28].

Alternative methods have been explored to tune the mechanical properties of GelMA using multiple crosslinking steps. For example, Rizwan et. al. used a sequential crosslinking approach in which a physical crosslinking step was performed by placing the gels at 4 °C prior to the photocrosslinking step [29]. In another study, Zhou et. al. used enzymatic crosslinking followed by photocrosslinking in order to improve the viscosity of GelMA for bioprinting purposes [30]. They mixed mTGase powder with GelMA and studied the viscoelastic properties of the constructed gels, resulting in better shear thinning properties and improved printability in extrusion-based printing [31]. Both studies demonstrated improved rheological properties of GelMA while enabling the fabrication of the hydrogels in predesigned shapes.

In this study, we introduced a different two-step crosslinking method, photocrosslinking followed by enzymatic crosslinking, in order to form dynamically tunable GelMA hydrogels with improved mechanical properties. First, photocrosslinking was used to construct the initial shape of the hydrogel. Then, using Ca²⁺ independent mTGase solution, the hydrogel was further crosslinked enzymatically, resulting in up to a seven-fold improvement in mechanical strength. The fabricated GelMA hydrogels were characterized in terms of compressive Young's modulus, rheology, swelling, degradation, and cell viability. Dual crosslinking strategies that are biocompatible and non-cytotoxic can potentially be used at any moment during the culture of the tissue engineered constructs. The ability to dynamically change the stiffness of the substrate would be beneficial in disease modeling applications where the stiffness of the tissue changes due to the disease pathology.

2. Results and Discussion

2.1. Methacrylation of Gelatin

GelMA was synthesized by incorporating methacrylate groups onto the amine containing side groups of gelatin (Figure 1a). The degree of methacrylation (DM) can be quantified by the percentage of the lysine groups that are substituted by the methacrylate groups, which was set to $52.5\% \pm 0.97\%$ in this study. The non-modified groups in GelMA serve as the sites for further enzymatic crosslinking by mTGase, which initiates a chemical reaction between glutamine and lysine groups within GelMA hydrogel (Figure 1c). This reaction improves the strength of the 3D hydrogels by providing extra support from the amide bonds.

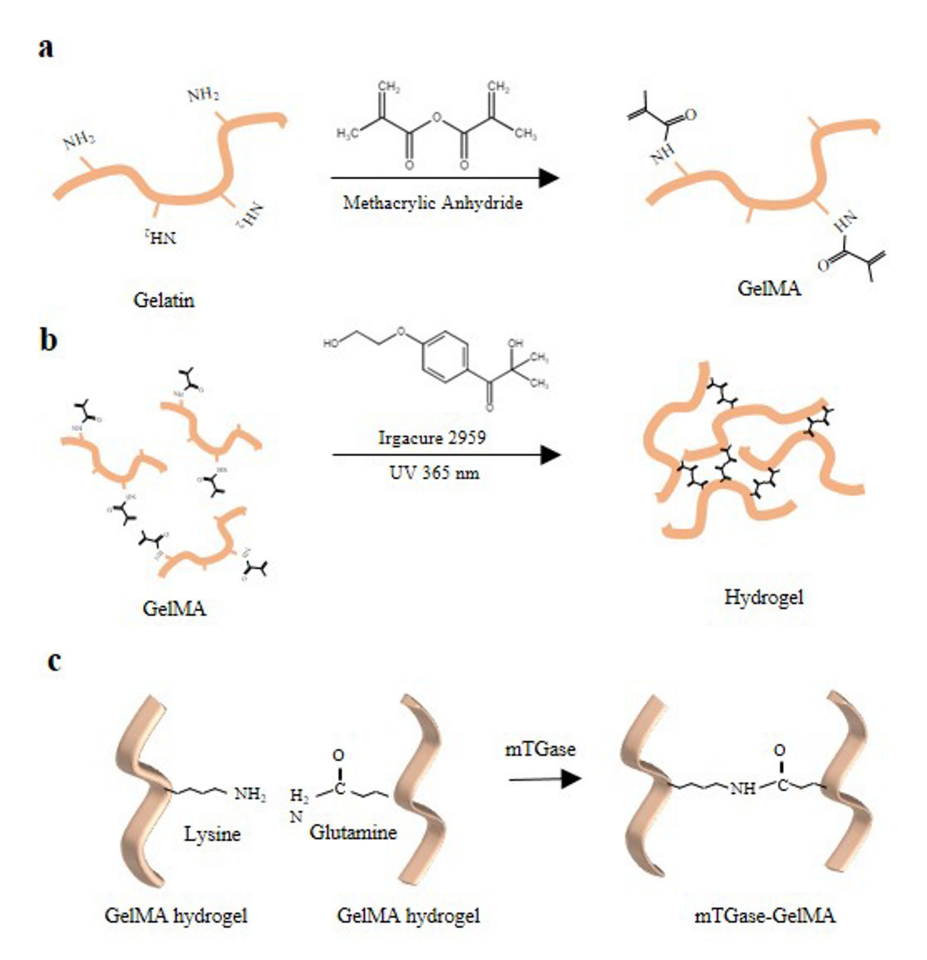


Figure 1. Schematic elucidating the crosslinking mechanism of GelMA (a) Modification of gelatin to GelMA (b) Photocrosslinking of GelMA hydrogel (c) Enzymatic crosslinking of GelMA hydrogel.

2.2. Rheological Characterization

To investigate the viscoelastic properties of the dual crosslinked gels, rheological characterization was performed using time sweep and frequency sweep tests. In the time sweep test, the storage and the loss modulus were recorded for 1 min and were found to be almost constant without mTGase treatment. With mTGase treatment, there was an increase in both the storage and the loss modulus for both 30 s and 60 s of UV photocrosslinking conditions (Figure 2a). The frequency sweep test showed a decrease in the storage modulus, whereas the loss modulus increased with the increasing frequency for both 30 s and 60 s of UV crosslinking conditions and with or without the mTGase treatment. Regardless of UV exposure time, the mTGase treatment increased the storage and the loss modulus (Figure 2b). For the lower frequency values, the storage modulus was greater than the loss modulus, which indicates predominantly elastic behavior rather than viscous behavior [32]. Our results showed that for 30 s of UV crosslinking condition, the gel structure was lost for single crosslinked gels, whereas mTGase treated gels retained their structure. Moreover, storage modulus indicates the ability to store deformation energy in an elastic manner and increases with the degree of crosslinking. Our results confirmed that the mTGase treatment increased the extent of crosslinking and enhanced the viscoelastic properties of the hydrogels.

Gels **2019**, *5*, 34
Gels **2019**, *4*, x FOR PEER REVIEW
4 of 14
4 of 14

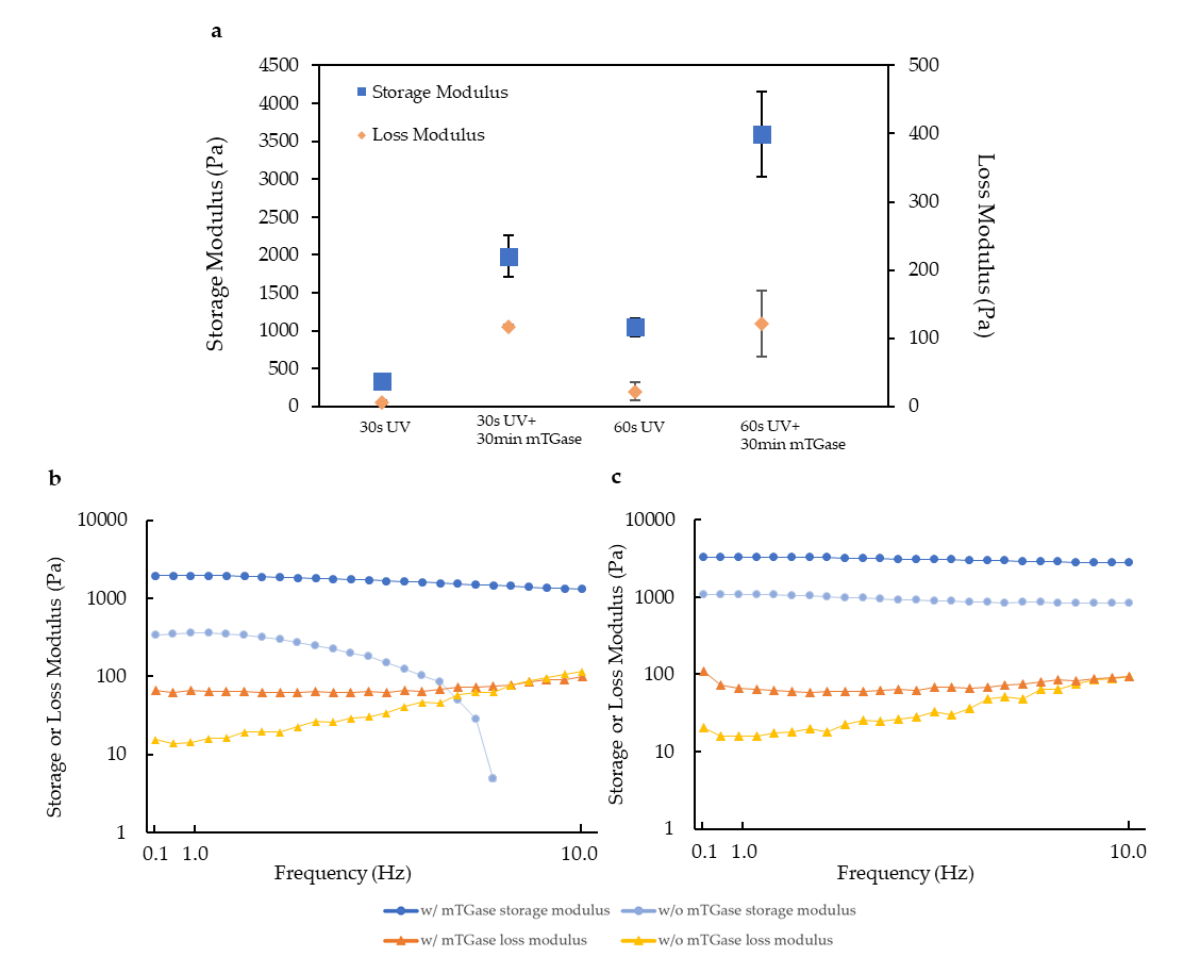


Figure 2. Viscoelastic properties of hydrogels crosslinked with 30 s and 60 s of UV exposure with or Figure 2. Viscoelastic properties in hydrogels crosslinked with 30 s and 60 s of UV exposure with or Figure 2. Viscoelastic properties in hydrogels crosslinked with 30 s and 60 s of UV exposure with or Figure 2. Viscoelastic properties of hydrogels crosslinked with 30 s and 60 s of UV exposure such 50 s of UV exposure conditions (w/s with; w/o: without; mTC assignments and transplantations).

mTGase: microbial transglutaminase). 2.3. Swelling and Mechanical Characterization

2.3. Swerling and Mechanical Charles was time as ured 1 day after incubation in phosphate-buffered saline

(PBS). Photocrosslinking alone, with 30 and 60 s of UV exposure, resulted in hydrogels that were The volume of the hydrogels was measured 1 day after incubation in phosphate buffered saline (PBS). Thorocrosslinking alone, with 30 and 60's of UV exposure, respectively. Thus, no significant exposure, resulted in hydrogels that were difference was observed between the two exposure times. On the contrary, when hydrogels were swollen by 18% (± 3%) and 22.1% (± 7%) of their initial volume, respectively. Thus, no significant further crosslinked with mTGase for 30 min right after UV crosslinking (dual crosslinking), they difference was observed between the two exposure times. On the contrary, when hydrogels were shrunk slightly, instead of swelling (Figure 3a). This is likely a result of increased crosslink levels further crosslinked with mTGase for 30 min right after UV crosslinking (dual crosslinking), they in the dual crosslinked hydrogels, which led to higher rigidity and lower water content. In parallel observed of crosslink (Figure 2a). The initial was result of increased crosslinking (Figure 2a). shrunk slightly, instead of swelling (Figure 3a). This is likely a result of increased crosslink levels in with the literature, the Young's modulus of the gels increased with increased UV treatment time [33]. the dual crosslinked hydrogels, which led to higher rigidity and lower water content. In parallel with Furthermore, stiffness test results showed that the treatment with milicase increased hydrogel stiffness the literature the Young's modulus of the gels increased with increased UV treatment time [33]. Furthermore, whiteens steat fresults feboused ethat, the treatment with until Gase are creased shydrogel stiffness proventoldifnea@stabUVofroslinkingexpaditionsaands2rfold. forial@soshilklingersalinking conditions afigureasing while gensignitis anterlifter on cerbety continual ourse some of his mathematical conditions affirm the second the conditions of the conditions are conditions affirm that we condition the conditions are conditions as the conditions of the conditions are conditionally as the condition of the conditions are conditionally as the condition of the c treated camples, when inhotocrassinked twith 30 costinuous of delyies, posturof was clossificad crosslinking was diskingetive atriveraning twilning a Catifficans of terval on obliving between an intension s. Floty maight which begins assisted by tetreat our partition of bloryge bandhees with circumstal problems. As of the control which to the increase apth for umbs linkings linked are up to whith mit charry linear phydrident bofMinuthenweenesdinecroprotorpoterminishoroical crosslitutional decreases of the gel and results in improved stiffness. As UV treatment time increases, the number of crosslinked groups occupied with methacrylic anhydride (MAnh) increases, therefore the potential for chemical crosslinking decreases.

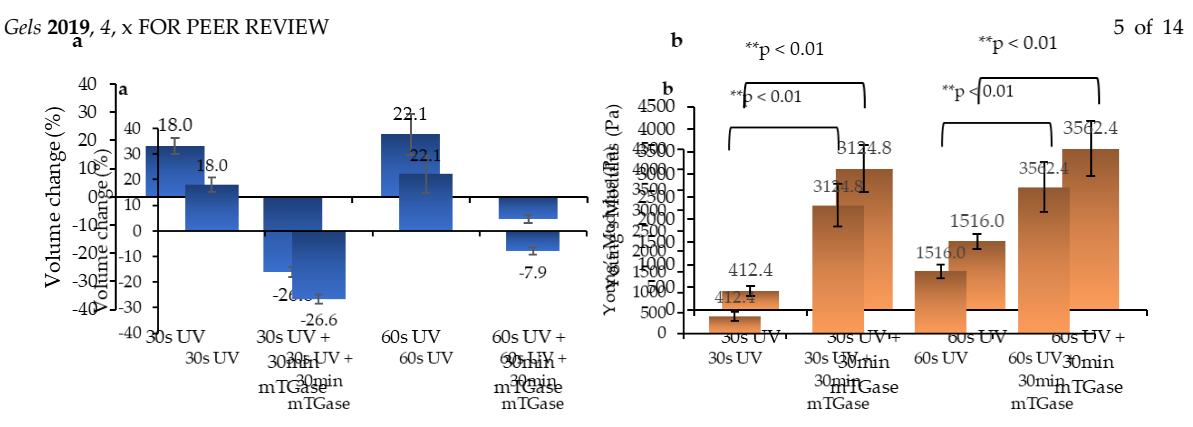


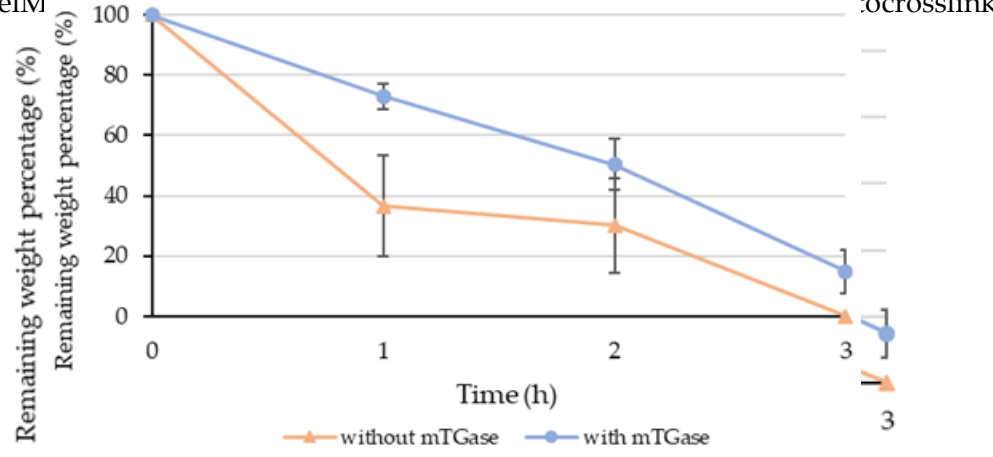
Figure 3. Swelling and mechanical characteristics of the gels (a) Swelling properties (b) Stiffgersmess Figure 3. Swelling properties (b) Stiffgersmess anal analysis using nanoingentation.

2.4. Degradation Test

2.4. DegradatidutiTasTest
To observe the effect of mTGase treatment on hydrogel degradation, collagenase digestion analysis

Troth Toxic pre-rained buffer the open for The sent treatment constructing about the construction and the construction of the cross reference of the cross of the cross of the construction of the cross of the c gels were performed the whereas 73.0% of the UV crosslinked gels remained, whereas 73.0%

of differential that after an hour only 36.6% of the leaves linked sets remained, whereas it was observed that after an hour only 36.6% of the CV crosslinked gels remained, whereas 74.8% of the differential that after an hour only 36.6% of the constituted gels remained, whereas 74.8% of the differential that the sets of gels remained. After 3 h, single crosslinked gels completely degraded, whereas the where the property of the constitute of the dual crosslinked by dropels still remained the different these results are consistent reas 14.8% of the dual crosslinked by dropels still remained this first at 1-these results are consistent. whereas 14.8% of the dual crosslinked hydrogels still remained (Figure 4). These results are consistent were as 14.8% of the dual crosslinked hydrogels still remained (Figure 4). These results are consistent with the diterature in the general free number of the control of t compared to GelM cocrosslinking [29].



Time (h) ls with or without mTGase treatment (mTGase: Figure 4. Enzymatic degradation of GelMA gelmore delma gelmore delma gelmore delma gelmore del delma gelma gelmore del delma gelma g microbial transglutaminase).

Figure 4: High water degradation of GelMA gels with or without mTGase treatment (mTGase: microbialdranes literating and be done for more complex shapes in larger dimensions. However, the UV crossfinking method usually requires a long exposure time or higher vimensions. 2.5. In waverathe Unity staling method usually requires a long exposure time or high UV intensity in obtain mechanically manageable hydrogel structures, which hargely inhibits hydrogel 3D printing in defining allong intensity applies along the forestime the function of the more than the printing and the first of the control of the first of the control of the contr obtain madianissifatetha affeable la Titase alestructures 30 la bighthat salvola history de l combinantid constituetal sons is tind of its blanche around interest to the constituent in the six a forest of the dual cross minimage that election the two confermed in the conferment of the conferment o

that the corners of the effect of MTC ase it earthean on 3D printed salingles as a proof of 3D model gridwhich is expected when printing with hydrogel materials. The brightfield images of the samples were shaped constructs consisting of two layers were printed. The printed shape is a square (10 mm × 10 taken immediately after printing. The samples were divided into three groups. The first group was mm), and the distance between the two neighboring lines is 2 mm. In all samples, it was observed that the corners of the squares were not as sharp and showed a slight discrepancy from the 3D model,

Gels 2019 that the corners of the squares were not as sharp and showed a slight discrepancy from the 3D model of 14 which is expected when printing with hydrogel materials. The brightfield images of the samples were onlyakhatacrosalinkedamith alla ağıdıra san pilk exposured The se cand groups was only enzypatically crosslipked by rusing kention and diagram of the constructs my interesting the constructs my interesting the constructs my interesting the constructs of the construction of the construct mT Case is a kettery and kept case is lead to inform all arein. The final ingular was dual crosslinked for the last 1917 Gyze sploution ampliktion in hit in centritier structumen. Plinet Good splonking swiasalfolds svirektely Enzytheratic crossishkingp/Theoresontpletionvetitheantine structure, hhdrowas slinking manufaticalled crossism kerticuith mTCass linking n That rapilty obsumed that they sando medically was only contantially by continued that they sando medically by and the contant of the conta SimmaTigs in solution did in or as 9 seliok parament which the seliots ustustive well-up and right of the land dipper PRS only bioink and soaked in him case so fution, greater distinguished by using geldting only ned This ink and soaked in intrase solution, greater disintegration occurred compared to the ones printed the bioink containing gelatin and nri Gase [34]. The remaining sample groups were kept in PBS with the bioink containing gelatin and mr Gase [34]. The remaining sample groups were kept in PBS with the bioink containing gelatin and mr Gase [34]. The remaining sample groups were kept in lution at 3. Covernight before taking the next set of images. Figure 5 shows the brightfield images PBS solution at 3. Covernight before taking the next set of images. Figure 5 shows the brightfield each group. Both treated and non-treated samples preserved their shapes and resolution. To images of each group. Both treated and non-treated samples preserved their shapes and resolution. investigate the effect of sample height, the same pattern was printed with six layers by following the lowestigate the effect of sample height, the same pattern was printed with six layers by following the previously described procedure. The results are shown in Figure 8 rightfield images showed that, immediately editer printing all the partners were similar. Also, the pore volume was preserved during printing a which is which disating in the construction of the cons pattentis preserved diluthe inesolution better in the mTGase treated cases solved bit 30 30 and 16d 50fs Df UV treatment that the mondital time, while how as wentified by measuring the clitistated between eighlighter lines in each of the clitistated between eighlighter lines in the clitistated between eighlighter lines in the clitistated by the clitistated between eighlighter lines in the clitistated by th on the theconordal sythis distance was measured as as from for the dual cross linked sand ble and 1.4 mmforther amplete the transplote the transplote the transplote the there are the same transplote that the the transplote the transplote transplote the transplote tra swelling of the hydrogel material, and thus the m Thase treatment enhanced the accuracy of the printing due to the the lower degree of swelling of the dual crosslinked hydrogels. printing due to the lower degree of swelling of the dual crosslinked hydrogels.

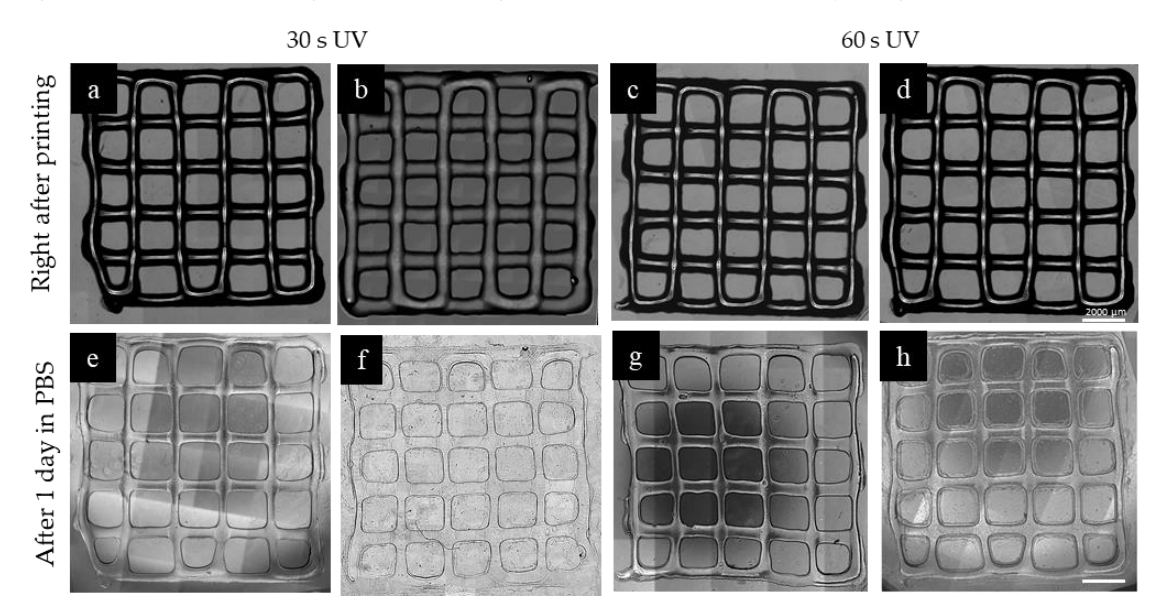


Figure 5. 3D printed constructs made of 2 layers, prepared using (a,b,e) 30 s of UV crosslinking without Figure 5. 3D printed constructs made of 2 layers, prepared using (a,b,e) 30 s of UV crosslinking mTGase treatment, (f) 30 s of UV crosslinking with 30 min mTGase treatment, (c,d,g) 60 s of UV crosslinking with 30 min mTGase treatment, (c,d,g) 60 s of UV crosslinking with 30 min mTGase treatment, (f) 30 s of UV crosslinking with 30 min mTGase treatment, (f) 30 s of UV crosslinking with 30 min mTGase treatment (f) 30 s of UV crosslinking with 30 min mTGase treatment (f) 30 s of UV crosslinking with 30 min mTGase treatment (f) 30 s of UV crosslinking with 30 s of UV crosslin

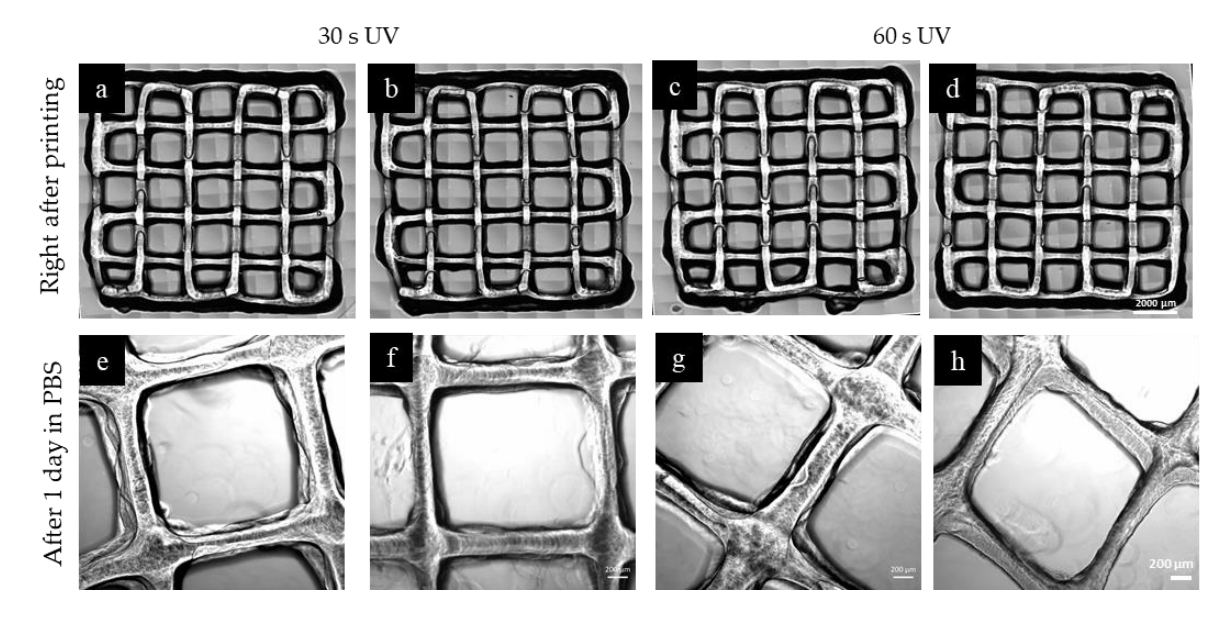


Figure 6. 3D printed constructs made of 6 layers, prepared using (a,b,e) 30 s of UV crosslinking without mTG ase treatment, (f) 30 s of UV crosslinking with 30 min mTGase treatment, (c,d,g) 60 of s UV without mTGase treatment, (f) 30 s of UV crosslinking with 30 min mTGase treatment, (c,d,g) 60 of s UV crosslinking with 30 min mTGase treatment, (c,d,g) 60 of s crosslinking without mTGase treatment, (h) 60 s of UV crosslinking with 30 min mTGase treatment. UV crosslinking without mTGase treatment, (h) 60 s of UV crosslinking with 30 min mTGase treatment. (Scale shows 2000 μm for upper row and 200 μm for lower row)

1.6. Cell Viability

 $2.6. \ \textit{Cell Viability}, \text{ human breast cancer cell line HCC1806}$

reliance the enterestic duar chost inking of deal staining, was performed and the centine in Conditions were compared. For each condition as amples (n = 3), were stained and the average was taken. No significant difference was observed for only photocrosslinked and dual crosslinked conditions were compared. For each condition, 3 samples (n = 3) were stained and the average was taken. No significant difference was observed between the dual crosslinked and photocrosslinked conditions for both 30 s and 60 s of UV exposure and the average was taken. No significant difference was observed duration (Figure 7a-d). For 30 s of UV exposure, the percentages of five cells were calculated as 86.7% ± between the dual crosslinked and photocrosslinked conditions for both 30 s and 60 s of UV exposure duration (Figure 7a-d). For 30 s of UV exposure, the percentages of five cells were calculated as 86.7% ± between the dual crosslinked and photocrosslinked conditions for both 30 s and 60 s of UV exposure duration (Figure 7a-d). For 30 s of UV exposure, the percentages of five cells were calculated as 86.7% ± 2.1% and 55.7% ± 4.1% of photocrosslinked and dual crosslinked conditions, respectively (Figure 7a-d). For the percentages of the cells were calculated as 86.7% ± 2.1% application for the percentages of the cells were calculated as 86.7% ± 2.1% application for the percentages of the cells were calculated as 86.7% ± 2.1% application for the percentages of the cells were calculated as 86.7% ± 2.1% application for the percentages of the cells were calculated as 86.7% ± 2.1% application for photocrosslinked and dual crosslinked conditions, respectively (Figure 7f). This result indicates That und That proposed the proposed for the cells were cells were conditions, respectively (Figure 7f). This result indicates That und That proposed for the cells and the cells and

The appropriate the patterns price of the patterns of the pattern of the patterns of the patterns of the patterns of the pattern of the patterns of the patte

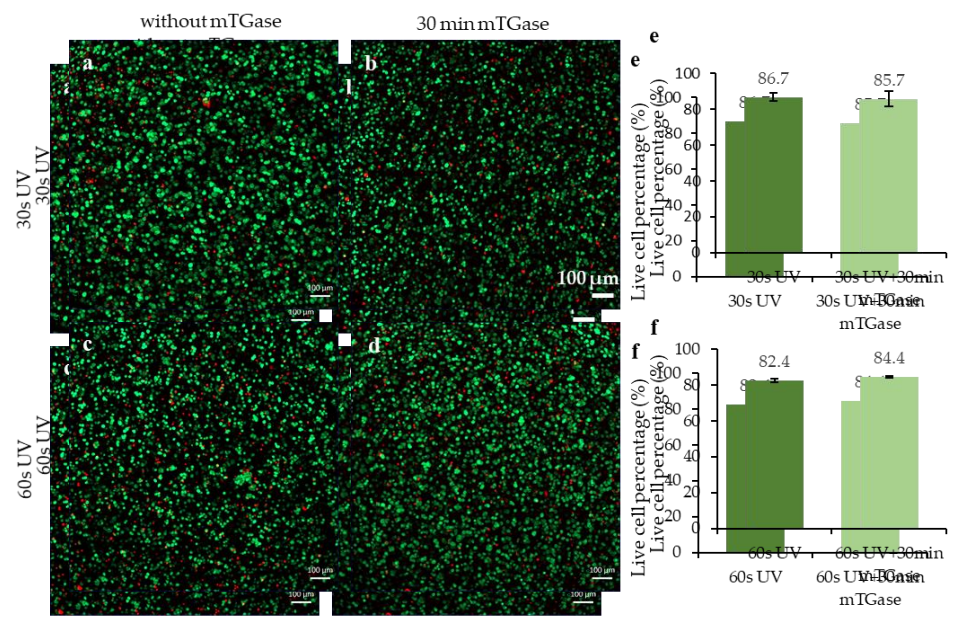


Figure 7. Cell viability analysis of cell-laden micropatterned gels prepared using (a) 30 s of UV Figure 7. Cell viability analysis of cell-laden micropatterned gels prepared using (a) 30 s of UV Figure 7. Cell viability analysis of cell-laden micropatterned gels prepared using (a) 30 s of UV Figure 7. Cell viability analysis of cell-laden micropatterned gels prepared using (a) 30 s of UV freatment with 30 min in Case treatment (c) 60 treatment with 30 min in Case treatment (d) 60 s of UV freatment with 30 min in Case treatment (e) live cell per centage comparison for 30 s of UV freatment with 30 min in Case treatment (e) live (e) live cell per centage comparison for 50 s of UV freatment with or without in Case treatment and (e) filive cell per centage comparison for 60 s of UV freatment with or without in Case treatment is need to be cell per centage comparison for 60 s of UV freatment with or without in Case treatment.

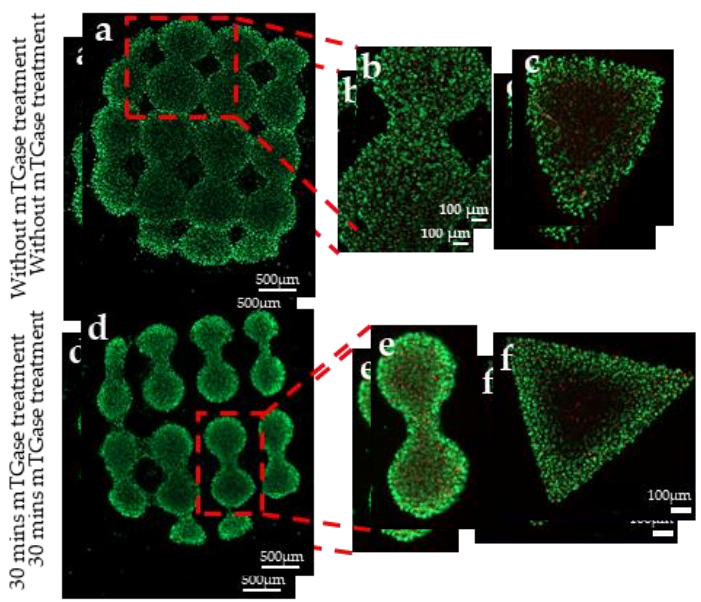


Figure 8. Micropatterned cell-laden gels created using photolithography (a) dumbbell patterns, Figure 8. Micropatterned cell-laden gels created using photolithography (a) dumbbell patterns (b) Figure 8. Micropatterned cell-laden gels created using photolithography (a) dumbbell patterns (b) Figure 8. Micropatterned cell-laden gels created using photolithography (a) dumbbell patterns, (b) zoomed in view zoomed dumbbell patterns, (e) zoomed in view

3. Codembrell pattern, (f) triangular pattern.

3. Conclusions
4. Conclusions
5. Conclusions
5. Conclusions
6. Con

Additionally, photopatterned as well as 3D printed gels retained their shapes better without affecting cell viability.

The second step of the presented dual crosslinking method can be applied at any time after initial photocrosslinking, and therefore can be used to mimic the dynamic stiffness changes which are common in many pathophysiological conditions such as cancer and heart attack.

4. Materials and Methods

4.1. Materials

MAnh, photo initiator (PI) Irgacure 2959, gelatin (gel strength 300g Bloom, Type A, from porcine skin) was purchased from Sigma-Aldrich (St. Louis, MO, USA). 12–14 kDa dialysis tube and Trypsin ethylenediamine tetraacetic acid (EDTA) were purchased from VWR (Chicago, IL, USA). Deuterium oxide (D_2O) was purchased from Cambridge Isotope Laboratories Inc (Andover, MA, USA). DMEM High Glucose and PBS were purchased from Corning (Corning, NY, USA). Fetal bovine serum (FBS) was purchased from Hyclone (South Logan, UT, USA) and penicillin-streptomycin (P) was purchased from Gibco (Waltham, MA, USA). Live/dead assay was purchased from Life Technologies (Carlsbad, CA, USA). The mTGase was a kind gift from Ajinomoto (Sunburg, MN, USA) and it has an enzymatic activity of 100 U/g.

4.2. Synthesize of GelMA

GelMA was synthesized by following the previously established protocol [38]. Briefly, 10 g of gelatin was dissolved in 100 mL of PBS at 60 °C. After completely dissolving, 2mL of MAnh was added dropwise and the solution was kept at 60 °C and left to react 3 h. After 3 h, 400 mL of PBS, pre-warmed to 40–50 °C, was added to the solution and mixed for 15 min. The solution was then transferred into a dialysis tube and dialyzed against deionized (DI) water at 40–50 °C with constant stirring. The dialysis was run for one week, with twice daily water changes. Finally, the GelMA solutions were filtered and lyophilized for further use.

4.3. Preparation and Crosslinking of Hydrogels

The hydrogel solution was prepared by dissolving GelMA (5% w/v) and adding PI (0.1% w/v in PBS). To dissolve GelMA in PBS, the mixture was kept in a water bath at 37 °C for 5 min. The solution was then transferred onto a stage with 100 μ m thick spacers and sandwiched between the stage and a glass slide. The gels were then exposed to 6.9 mW/cm² UV irradiation by using a UV lamp (Lumen Dynamics, (Mississauga, ON, Canada). As a result, circular shaped gels were obtained. The hydrogels were prepared at room temperature, and immediately placed in 37 °C.

The mTGase solution was prepared with DI water (80 mg/mL w/v). The solution was mixed thoroughly using a vortex and kept at 37 °C to provide complete dissolution of mTGase. The gels were prepared using the conditions shown in Table 1. To determine the effect of treatment time, two different time points were tried: the gels were soaked in mTGase solution for 30 min and overnight. It was observed that 30 min treatment improved the mechanical properties, whereas the overnight application decreased them. Further optimization can be performed in future studies to find the best enzyme treatment conditions.

Table 1. Parameters used for gel preparation.

UV Treatment Time (s)	mTGase Treatment Time (min)
30	-
30	30
60	-
60	30

4.4. Materials Characterization

4.4.1. ¹H NMR Characterization

The methacrylation of gelatin was characterized with an ^{1}H NMR spectroscopy. GelMA solution was prepared with a concentration of 30 mg/mL in $D_{2}O$ and ^{1}H NMR spectra were collected. After baseline correction, the areas of the peaks were integrated. The degree of methacrylation, which is the percentage of ε -amino groups of gelatin modified with MAnh, was calculated by using Equation (1).

$$DM(\%) = 1 - \frac{GelMA \text{ lysine methylene area}}{Gelatin \text{ lysine metylene area}}$$
(1)

4.4.2. Rheological Properties

Two different rheological tests were conducted to characterize the viscoelastic properties of the only photocrosslinked and dual crosslinked gels. For both experiments, 8 mm diameter parallel-plate geometry was used with a crosshatch plate. A time sweep test was done to study the strength of the structure of the gels. For this test, storage modulus (G') and loss modulus (G") were recorded as a function of time under a fixed frequency of 1 Hz and strain of 3%. Each gel was tested at 37 °C for 1 min. During testing, measurements were taken every 10 s and the average of six data points shows the average modulus of each gel.

The frequency sweep test was done to observe the viscoelastic properties of the gels. The storage modulus and loss modulus were recorded over a frequency range from 0.1 to 10 Hz with 2% strain at 37 °C.

4.4.3. Mechanical Properties

To determine the mechanical properties, compression stiffness test was conducted by using a nanoindenter (Optics 11, Westwood, MA, USA) with an indentation probe (spring constant of $0.45 \, \text{N/m}$, tip diameter of $50 \, \mu \text{m}$). Young's modulus of each hydrogel was calculated using in house MATLAB code, which determines the slope of the stress-strain plot in the elastic region.

4.4.4. Swelling Test

The swelling properties of hydrogels were measured by observing the volume changes between the hydrogels that were freshly prepared and those that were incubated in PBS solution for 24 h. The volumes of the gels were calculated by multiplying the surface area with the thickness. To calculate the surface area, images of the gels (n = 3) were taken immediately after preparation and on the next day and measured with ImageJ (version 1.51k, National Institutes of Health Bethesda, MD, USA). The thickness of the gels was 1 mm right after preparation, which was decided by the height of the stage used for hydrogel fabrication. One day after fabrication, the thickness of the gels was determined by the force reading in the rheometer. The upper head of the rheometer was lowered until it touched the surface of the gel. At the contact point, the force reading started increasing. The point when the force reading started increasing from zero was used as the contact point to decide the thickness of each gel.

4.4.5. Degradation Test

For the degradation test, the hydrogel solution was prepared by dissolving GelMA (5% w/v) and adding PI (0.1% w/v in PBS). From this solution, 30 μ l disks were prepared using PDMS molds 6 mm in diameter and 1 mm thick, then crosslinked with either only 30 s UV exposure or 30 s UV exposure followed by 30 min mTGase (80 mg/mL w/v in DMEM) treatment. After polymerization, the hydrogel discs were transferred to 24-well plates and allowed to swell in DMEM medium supplemented with FBS and penicillin in an incubator at 37 °C overnight. The next day, the medium was removed and 1 mL of collagenase type 2 (240 U/mg, Worthington Biochemical, Lakewood, NJ, USA) with 5 U/mL

concentration in DMEM was added to each well. The weight of the hydrogels was measured after carefully drying with a delicate tissue wipe (KimTech Science, Roswell, GA, Canada), every hour for 3 h. For each time point, 3 samples were used, and the remaining weight (RW) percentage was calculated using Equation (2).

RW (%) =
$$100 + \frac{\text{(weight at required time point - initial weight)}}{\text{initial weight}} * 100$$
 (2)

4.4.6. 3D Printing

For 3D printing, bioink was prepared by dissolving GelMA ($10\% \ w/v$) in PBS and adding PI ($0.1\% \ w/v$ in PBS). The bioink was then transferred into the cartridge while it was still liquid. The cartridge was put in 4 °C for 5 min to achieve the required viscosity prior to printing. A CELLINK Inkredible+ Bioprinter was used for printing. Printing was done at room temperature, with a pressure range of 50–57 kPa. The translational speed of the nozzle was 75 mm/min and the nozzle diameter was 250 μ m. By using a custom-made G-code, a grid pattern consisting of two layers with dimensions of 1 cm \times 1 cm was printed into each well of a 12-well plate. Printed constructs were either treated with 30 s or 60 s UV only, or they went through mTGase treatment for 30 min following the UV crosslinking. All samples were kept at 37 °C in PBS solution overnight. Brightfield images were taken right after fabrication as well as 24 h after incubation.

4.5. Cell encapsulation and Imaging

4.5.1. Cell Encapsulation for Biocompatibility

Human breast cancer cell line HCC1806 cells were cultured in DMEM high glucose supplemented with 10% FBS and 1% P/S at 37 °C with 5% CO₂. Cells were collected when they reached approximately 80% confluency and encapsulated in GelMA hydrogels (n=3) with a cell density of 0.1 million cells per construct (5µL total volume). The hydrogel solution was prepared by dissolving GelMA (5% w/v) in PBS and mixing in PI to achieve a final concentration of 0.1% w/v. Then, the solution was mixed with cell suspension at a ratio of 1:1 (GelMA:cell solution). The mixture was then transferred onto a stage with 100 µm thick spacers and sandwiched between the stage and a glass slide. The whole structure was exposed to 6.9 mW/cm² UV irradiation for 30 or 60 s. The amount of PI and the dose of UV exposure have been shown to be harmless for cell encapsulation studies [38]. The hydrogels were washed thoroughly with PBS to remove the excess PI. The mTGase solution was prepared with culture media (80 mg/mL w/v). The solution was mixed thoroughly using a vortex and kept at 37 °C to provide complete dissolution of mTGase. After washing, half of the samples were kept in mTGase solution at 37 °C for 30 min. After 30 min the mTGase solution was replaced with fresh culture media.

To determine the cell viability, cells were stained with Live/Dead Assay (Life technologies) 24 h after encapsulation, following the manufacturer's instructions. Live cells were stained with Calcein AM (green), and dead cells were stained with Ethidium homodimer-1 (red). The images were taken with a fluorescence microscope (Zeiss, Hamamatsu ORCA flash 4.0, Thornwood, NY, USA). For each hydrogel, z-serial images were taken at three different locations with optical sectioning, and the background signals were eliminated with structural illumination (Apotome, Zeiss, Thornwood, NY, USA). Live and dead cells were counted in ImageJ software. Live cell percentage was calculated by using Equation (3).

Live cell (%) =
$$[(live cell number)/(total cell number)] * 100$$
 (3)

4.5.2. Cell Encapsulation for Photolithography

For photolithography test, gels were prepared by using the same GelMA and PI concentrations as described above and mixed with 20 million cells/mL. The mixture was then transferred onto a stage

with 100 μ m thick spacers and sandwiched between the stage and a glass slide. A photomask with the desired micropatterns was placed on top of the glass slide and exposed to 6.9 mW/cm² UV irradiation for 60 s by using a UV lamp (Lumen Dynamics, Mississauga, ON, Canada).

Author Contributions: Conceptualization, G.B., X.Y. and P.Z.; methodology, G.B., X.Y. and P.Z.; validation, G.B., X.Y. and P.Z.; formal analysis, G.B. and X.Y.; investigation, G.B.; resources, P.Z.; data curation, G.B. and X.Y.; writing—original draft preparation, G.B.; writing—review and editing, G.B., X.Y. and P.Z.; visualization, G.B.; supervision, P.Z.; funding acquisition, P.Z.

Funding: This research was funded by NSF-CAREER Award # 1651385, NSF Award # 1805157 and NIH Award # 1 R01 HL141909.

Conflicts of Interest: The authors declare no conflict of interest.

References

- 1. Ding, Z.Z.; Ma, J.; He, W.; Ge, Z.L.; Lu, Q.; Kaplan, D.L. Simulation of ECM with silk and chitosan nanocomposite materials. *J. Mater. Chem. B* **2017**, *5*, 4789–4796. [CrossRef] [PubMed]
- 2. Calle, E.A.; Hill, R.C.; Leiby, K.L.; Le, A.V.; Gard, A.L.; Madri, J.A.; Hansen, K.C.; Niklason, L.E. Targeted proteomics effectively quantifies differences between native lung and detergent-decellularized lung extracellular matrices. *Acta Biomater.* **2016**, *46*, 91–100. [CrossRef] [PubMed]
- 3. Chen, G.; Chen, J.; Yang, B.; Li, L.; Luo, X.; Zhang, X.; Feng, L.; Jiang, Z.; Yu, M.; Guo, W.; et al. Combination of aligned PLGA/Gelatin electrospun sheets, native dental pulp extracellular matrix and treated dentin matrix as substrates for tooth root regeneration. *Biomaterials* **2015**, *52*, 56–70. [CrossRef] [PubMed]
- 4. Lu, P.; Takai, K.; Weaver, V.M.; Werb, Z. Werb Extracellular Matrix Degradation and Remodeling in Development and Disease. *Cold Spring Harb. Perspect. Biol.* **2011**, *3*, a005058. [CrossRef] [PubMed]
- 5. He, Y.; Lu, F. Development of Synthetic and Natural Materials for Tissue Engineering Applications Using Adipose Stem Cells. *Stem Cells Int.* **2016**, *2016*, *5786257*. [CrossRef]
- 6. Noori, A.; Ashrafi, S.J.; Vaez-Ghaemi, R.; Hatamian-Zaremi, A.; Webster, T.J. A review of fibrin and fibrin composites for bone tissue engineering. *Int. J. Nanomed.* **2017**, 12, 4937–4961. [CrossRef]
- 7. Lutolf, M.P.; Hubbell, J.A. Synthetic biomaterials as instructive extracellular microenvironments for morphogenesis in tissue engineering. *Nat. Biotechnol.* **2005**, *23*, 47–55. [CrossRef]
- 8. Chaudhari, A.; Vig, K.; Baganizi, D.; Sahu, R.; Dixit, S.; Dennis, V.; Singh, S.; Pillai, S. Future Prospects for Scaffolding Methods and Biomaterials in Skin Tissue Engineering: A Review. *Int. J. Mol. Sci.* **2016**, *17*, 1974. [CrossRef]
- 9. Nichol, J.W.; Koshy, S.T.; Bae, H.; Hwang, C.M.; Yamanlar, S.; Khademhosseini, A. Cell-laden microengineered gelatin methacrylate hydrogels. *Biomaterials* **2010**, *31*, 5536–5544. [CrossRef]
- 10. Lee, B.; Lum, N.; Seow, L.; Lim, P.; Tan, L. Tan Synthesis and Characterization of Types A and B Gelatin Methacryloyl for Bioink Applications. *Materials* **2016**, *9*, 797. [CrossRef]
- 11. Yue, K.; Trujillo-de Santiago, G.; Alvarez, M.M.; Tamayol, A.; Annabi, N.; Khademhosseini, A. Synthesis, properties, and biomedical applications of gelatin methacryloyl (GelMA) hydrogels. *Biomaterials* **2015**, *73*, 254–271. [CrossRef] [PubMed]
- 12. Aubin, H.; Nichol, J.W.; Hutson, C.B.; Bae, H.; Sieminski, A.L.; Cropek, D.M.; Akhyari, P.; Khademhosseini, A. Directed 3D cell alignment and elongation in microengineered hydrogels. *Biomaterials* **2010**, *31*, 6941–6951. [CrossRef] [PubMed]
- 13. Yin, J.; Yan, M.; Wang, Y.; Fu, J.; Suo, H. 3D Bioprinting of Low-Concentration Cell-Laden Gelatin Methacrylate (GelMA) Bioinks with a Two-Step Cross-linking Strategy. *Acs Appl. Mater. Interfaces* **2018**, *10*, 6849–6857. [CrossRef] [PubMed]
- 14. Colosi, C.; Shin, S.R.; Manoharan, V.; Massa, S.; Costantini, M.; Barbetta, A.; Dokmeci, M.R.; Dentini, M.; Khademhosseini, A. Microfluidic Bioprinting of Heterogeneous 3D Tissue Constructs Using Low-Viscosity Bioink. *Adv. Mater.* **2016**, *28*, 677–684. [CrossRef] [PubMed]
- 15. Liu, W.; Heinrich, M.A.; Zhou, Y.; Akpek, A.; Hu, N.; Liu, X.; Guan, X.; Zhong, Z.; Jin, X.; Khademhosseini, A.; et al. Extrusion Bioprinting of Shear-Thinning Gelatin Methacryloyl Bioinks. *Adv. Healthc. Mater.* **2017**, *6*, 1601451. [CrossRef] [PubMed]

16. Visser, J.; Melchels, F.P.; Jeon, J.E.; Van Bussel, E.M.; Kimpton, L.S.; Byrne, H.M.; Dhert, W.J.; Dalton, P.D.; Hutmacher, D.W.; Malda, J. Reinforcement of hydrogels using three-dimensionally printed microfibres. *Nat. Commun.* **2015**, *6*, 6933. [CrossRef] [PubMed]

- 17. Wang, H.; Zhou, L.; Liao, J.; Tan, Y.; Ouyang, K.; Ning, C.; Ni, G.; Tan, G. Cell-laden photocrosslinked GelMA–DexMA copolymer hydrogels with tunable mechanical properties for tissue engineering. *J. Mater. Sci. Mater. Med.* **2014**, 25, 2173–2183. [CrossRef]
- 18. Das, S.; Pati, F.; Choi, Y.J.; Rijal, G.; Shim, J.H.; Kim, S.W.; Ray, A.R.; Cho, D.W.; Ghosh, S. Bioprintable, cell-laden silk fibroin–gelatin hydrogel supporting multilineage differentiation of stem cells for fabrication of three-dimensional tissue constructs. *Acta Biomater.* **2015**, *11*, 233–246. [CrossRef]
- 19. Camci-Unal, G.; Cuttica, D.; Annabi, N.; Demarchi, D.; Khademhosseini, A. Synthesis and Characterization of Hybrid Hyaluronic Acid-Gelatin Hydrogels. *Biomacromolecules* **2013**, *14*, 1085–1092. [CrossRef]
- 20. Shin, H.; Olsen, B.D.; Khademhosseini, A. The mechanical properties and cytotoxicity of cell-laden double-network hydrogels based on photocrosslinkable gelatin and gellan gum biomacromolecules. *Biomaterials* **2012**, *33*, 3143–3152. [CrossRef]
- 21. Shin, S.R.; Bae, H.; Cha, J.M.; Mun, J.Y.; Chen, Y.C.; Tekin, H.; Shin, H.; Farshchi, S.; Dokmeci, M.R.; Tang, S.; et al. Carbon Nanotube Reinforced Hybrid Microgels as Scaffold Materials for Cell Encapsulation. *ACS Nano* 2012, 6, 362–372. [CrossRef] [PubMed]
- 22. Shin, S.R.; Jung, S.M.; Zalabany, M.; Kim, K.; Zorlutuna, P.; Kim, S.B.; Nikkhah, M.; Khabiry, M.; Azize, M.; Kong, J.; et al. Carbon-Nanotube-Embedded Hydrogel Sheets for Engineering Cardiac Constructs and Bioactuators. *ACS Nano* 2013, 7, 2369–2380. [CrossRef] [PubMed]
- 23. Serafim, A.; Tucureanu, C.; Petre, D.G.; Dragusin, D.M.; Salageanu, A.; Van Vlierberghe, S.; Dubruel, P.; Stancu, I.C. One-pot synthesis of superabsorbent hybrid hydrogels based on methacrylamide gelatin and polyacrylamide. Effortless control of hydrogel properties through composition design. *New J. Chem.* **2014**, *38*, 3112–3126. [CrossRef]
- 24. Cha, C.; Shin, S.R.; Gao, X.; Annabi, N.; Dokmeci, M.R.; Tang, X.; Khademhosseini, A. Controlling Mechanical Properties of Cell-Laden Hydrogels by Covalent Incorporation of Graphene Oxide. *Small* **2014**, *10*, 514–523. [CrossRef] [PubMed]
- 25. Hutson, C.B.; Nichol, J.W.; Aubin, H.; Bae, H.; Yamanlar, S.; Al-Haque, S.; Koshy, S.T.; Khademhosseini, A. Synthesis and Characterization of Tunable Poly (Ethylene Glycol): Gelatin Methacrylate Composite Hydrogels. *Tissue Eng. Part A* **2011**, *17*, 1713–1723. [CrossRef] [PubMed]
- Daniele, M.A.; Adams, A.A.; Naciri, J.; North, S.H.; Ligler, F.S. Interpenetrating networks based on gelatin methacrylamide and PEG formed using concurrent thiol click chemistries for hydrogel tissue engineering scaffolds. *Biomaterials* 2014, 35, 1845–1856. [CrossRef] [PubMed]
- 27. Hasan, A.; Khattab, A.; Islam, M.A.; Hweij, K.A.; Zeitouny, J.; Waters, R.; Sayegh, M.; Hossain, M.M.; Paul, A. Injectable Hydrogels for Cardiac Tissue Repair after Myocardial Infarction. *Adv. Sci.* **2015**, *2*, 1500122. [CrossRef]
- 28. Plodinec, M.; Loparic, M.; Monnier, C.A.; Obermann, E.C.; Zanetti-Dallenbach, R.; Oertle, P.; Hyotyla, J.T.; Aebi, U.; Bentires-Alj, M.; Lim, R.Y.; et al. The nanomechanical signature of breast cancer. *Nat. Nanotechnol.* **2012**, *7*, 757–765. [CrossRef]
- 29. Rizwan, M.; Peh, G.S.; Ang, H.P.; Lwin, N.C.; Adnan, K.; Mehta, J.S.; Tan, W.S.; Yim, E.K. Sequentially-crosslinked bioactive hydrogels as nano-patterned substrates with customizable stiffness and degradation for corneal tissue engineering applications. *Biomaterials* **2017**, *120*, 139–154. [CrossRef]
- 30. Zhou, M.; Lee, B.H.; Tan, L.P. A dual crosslinking strategy to tailor rheological properties of gelatin methacryloyl. *Int. J. Bioprint.* **2017**, *3*, 130–137. [CrossRef]
- 31. Zhou, M.; Lee, B.H.; Tan, Y.J.; Tan, L.P. Microbial transglutaminase induced controlled crosslinking of gelatin methacryloyl to tailor rheological properties for 3D printing. *Biofabrication* **2019**, *11*, 025011. [CrossRef] [PubMed]
- 32. Kumar, A.; Lee, Y.; Kim, D.; Rao, K.M.; Kim, J.; Park, S.; Haider, A.; Han, S.S. Effect of crosslinking functionality on microstructure, mechanical properties, and in vitro cytocompatibility of cellulose nanocrystals reinforced poly (vinyl alcohol)/sodium alginate hybrid scaffolds. *Int. J. Biol. Macromol.* **2017**, *95*, 962–973. [CrossRef] [PubMed]

33. O'Connell, C.D.; Zhang, B.; Onofrillo, C.; Duchi, S.; Blanchard, R.; Quigley, A.; Bourke, J.; Gambhir, S.; Kapsa, R.; Di Bella, C.; et al. Tailoring the mechanical properties of gelatin methacryloyl hydrogels through manipulation of the photocrosslinking conditions. *Soft Matter* 2018, *14*, 2142–2151. [CrossRef] [PubMed]

- 34. Irvine, S.A.; Agrawal, A.; Lee, B.H.; Chua, H.Y.; Low, K.Y.; Lau, B.C.; Machluf, M.; Venkatraman, S. Printing cell-laden gelatin constructs by free-form fabrication and enzymatic protein crosslinking. *Biomed. Microdevices* **2015**, *17*, 16. [CrossRef] [PubMed]
- 35. Billiet, T.; Gevaert, E.; De Schryver, T.; Cornelissen, M.; Dubruel, P. The 3D printing of gelatin methacrylamide cell-laden tissue-engineered constructs with high cell viability. *Biomaterials* **2014**, *35*, 49–62. [CrossRef] [PubMed]
- 36. Yang, G.; Xiao, Z.; Ren, X.; Long, H.; Qian, H.; Ma, K.; Guo, Y. Enzymatically crosslinked gelatin hydrogel promotes the proliferation of adipose tissue-derived stromal cells. *Peer J.* **2016**, *4*, e2497. [CrossRef] [PubMed]
- 37. Cates, R.S. Influence of Crosslink Density on Swelling and Conformation of Surface-Constrained Poly(*N*-Isopropylacrylamide) Hydrogels. Master's Thesis, University of South Florida, Tampa, FL, USA, 2010.
- 38. Yue, X.; Nguyen, T.D.; Zellmer, V.; Zhang, S.; Zorlutuna, P. Stromal cell-laden 3D hydrogel microwell arrays as tumor microenvironment model for studying stiffness dependent stromal cell-cancer interactions. *Biomaterials* **2018**, *170*, 37–48. [CrossRef]



© 2019 by the authors. Licensee MDPI, Basel, Switzerland. This article is an open access article distributed under the terms and conditions of the Creative Commons Attribution (CC BY) license (http://creativecommons.org/licenses/by/4.0/).